On the Earthquake Resistance of Anchored Sheet-Pile Bulkheads

by Susumu Kurata*, Hideo Arai* and Toshiyuki Yokoi*

Introduction

It has been reported[1] that most earthquake damages of sheet-pile bulkheads were displacements of the top due to the shortage of the anchor resistance, and that only a few destructions were caused by sliding of the embedded portion or the excess bending moment against the wall. Such characteristic of earthquake damages seems to be explained qualitatively by the static properties of sheet-pile walls, which have been obtained up to date, and by the vibration characteristics of soil near the surface. The soil around the anchored sheet-pile wall is under a complicated confining condition, since the earthpressure depends to large extent on the confining condition of soil, it is not easy to analyse the behaviour of such a structure during earthquakes.

Most of sheet-pile bulkheads are the water-front structures, however, as the first step of the investigation, the vibration tests of model anchored sheet-pile walls were performed in the dry state. Such tests using a vibration table do not always correspond to the state of the structures during earthquakes, because the earthquake motion is the waves which propagate through the earth. However, the general tendency of the behaviour of structures in vibration can be seen from the results of experiments and it may be possible to investigate the seismic stability of complicated earthstructures such as sheet-pile walls.

Experiments

The experiments were performed in a box on the vibration table. The vibration table used in this test was the same as that used in previous studies of "Lateral Earthpressure in an Earthquake".[2] It is impossible to analyse strictly the movement of sand particles in the box, because the aggregation of sand particles in the vibration box is the non-holonomic system in a dynamical point of view. However, the tests can be performed easily under the wide range of test conditions and the investigation of the characteristic behaviour of earthstructures during vibrations can be made.

The model similarity by the dimensional analysis is considered mainly for the wall. Test conditions for the sand shall be considered later under the examination of test results, since there are many unknown factors in the behaviour of the soil in vibration.

Anchored sheet-pile bulkheads resist against the loads by the bending stiffness of the wall, the resistance of the anchor and the resistance of

---

* Port and Harbour Technical Research Institute, Ministry of Transportation, Japan.

a embedded portion of the wall. The behaviour of anchored sheet-pile walls without earthquakes may be represented by the theory established by P.W. Rowe.[3] According to his theory, if the fundamental equation governing the flexure of a beam supported by sand is,

$$EI\frac{d^4y}{dx^4} = p_x - m\frac{xy}{D}$$

then the bending moments of the wall can be represented as follows.

$$M = K_a\gamma H^3 \cdot f(\alpha, \beta, \delta, m\rho, \varepsilon)$$

where Ka is the active earthpressure coefficient, γ the soil density, δ_s the surcharge pressure ($\delta = \delta_s/\gamma H$), m the soil stiffness modulus, $\rho = H^4/EI$ the flexibility number, and α, β, ε are the geometrical dimensions indicated in Fig.1. In reference to Rowe's theory, the bending moments for a unit width of the wall during vibration can be expressed by the following function.

$$M = f(T, W, P, m, EI, g, H) \qquad (1)$$

where T (sec) is the vibration period, W ($kg\cdot cm^{-1}$) the weight of the wall, P ($kg\cdot cm^{-2}$) the load acting on the wall, m ($kg\cdot cm^{-3}$) the soil stiffness modulus, EI ($kg\cdot cm$) the flexural rigidity of the wall, g ($cm\cdot sec^{-2}$) the acceleration of the gravity, H (cm) the height of the wall. Applying the dimensional analysis to eq.(1), the following equation is obtained.

$$M = \frac{EI}{H}\cdot f\left(\frac{T^2 g}{H}, \frac{W\rho}{H^2}, \frac{P\rho}{H}, m\rho\right) \qquad (2)$$

And the law of similarity becomes as follows.

$$\left(\frac{T_m}{T_p}\right)^2\left(\frac{H_p}{H_m}\right) = \left(\frac{W_m}{W_p}\right)\left(\frac{\rho_m}{\rho_p}\right)\left(\frac{H_p}{H_m}\right)^2 = \left(\frac{P_m}{P_p}\right)\left(\frac{\rho_m}{\rho_p}\right)\left(\frac{H_p}{H_m}\right) = \left(\frac{m_m}{m_p}\right)\left(\frac{\rho_m}{\rho_p}\right) \qquad (3)$$

First two terms of eq.(3) are the quantities concerned with the wall only, and last two terms are the quantities concerned with both the wall and the soil. As the characteristic quantities on the wall are comparatively well known, it is easy to make the similar model wall to the prototype.
But the quantities on the sand are not evident on the prototype and it is quite difficult to make the similar model condition on sand to the prototype.

A steel model and an aluminium model with a height H=1.1m and ζ =9.18 $\times 10^3$ cm^{-2}·kg, 11.63$\times 10^3$ cm^{-2}·kg respectively were made, corresponding to the Z-type sheet-pile wall with a height H=20cm and ζ =9.3$\times 10^3$ cm^{-2}·kg as the prototype. These models did not strictly satisfy the condition of similarity, and especially the steel model wall was considerably heavy. As the load acting on the wall and the subsoil stiffness are the quantities on the sand, it is difficult to determine them uniquely. Also it is difficult to decide which period should be taken as Tp, but it is assumed to be 1.0 ~ 2.0 sec for the present purpose.

In tests, the model wall was placed in the central part of the vibration box which was 4m long, 1m wide and 1.5m high, and anchored as shown in Fig.1. The dry sand (the uniformity coefficient : 1.503=0.185mm/0.123 mm, the angle of repose : 32.5°) was filled in the box as the backfill and the subsoil. Two sorts of vibration with the period of 0.3 sec were given. One was the increasing vibration, acceleration of which was increased to about 200 ~ 350 gal at constant rate of about 1 gal per 1 period, and the other was the solitary vibration which had the properties like a shock.

The strain of the wall was measured by strain gauges, and the deflection of the wall above the dredge level by dial gages in the static state and the differential transformers in the vibration, and the anchor load by the magnetostriction type load cells. They were recorded by the electromagnetic oscillograph during vibration.

Results of Experiments

Before the vibration, external forces, namely the earthpressure and the surcharge are acting on the wall, so that the wall, the anchor rod and the soil in front of the embedded wall are being stressed. When the vibration is given, the external force due to vibration is added to that state, and the internal stresses of the structure are changed. The change of stresses relates to both the state before the vibration and the characteristics of the vibration.

Increasing vibration

As the representative examples, the variations of the strains of the wall, the displacements of the wall and the anchor loads at 150 gal of the table acceleration in the increasing vibration are shown in Figs.2 (1), (2).

(1) Bending moments against the wall

The bending moments were obtained by the strain measurements. The distributions of the bending moment are shown in Figs.4 (1), (2), (3). The maximum bending moment is observed to take place at the middle part of the span between the anchorage and the dredge level, and its magnitude increases with the increasing acceleration of vibration. The variations of the bending moments during vibrations consist of two parts, one part is oscillating with same period as the forced vibration, and the other part changes statically between the values of before and after vibrations. The statically changing part is remarkably large, on the other hand, the

oscillating part is extremely small. Though the stiffness of soil in front of the embedded wall tends to decrease with the increasing acceleration of vibration, the bending moment in the embedded portion of the wall increases when the value of the soil stiffness modulus is higher than a critical value, and decreases when the modulus is lower than a critical value. The critical value of the soil stiffness modulus is about 3 $kg \cdot cm^{-3}$ in the present experiments. When the soil stiffness modulus is equal to the critical value, the point of the zero bending moment coincides with the dredge level. This fact seems to be interesting in connection with the fixity of the embedment.

The curves in the figures are the values calculated from the Rowe's theory by taking the parameter m_f so as to fit to the measured values. It is noticed that the general tendency of experiments coincides with the theory. Since the bending moment is governed principally by the intensity of the surcharge, the degree of the fixity in the embedded portion and the loads acting against the wall, it is convenient to discuss the results by investigating the following earthpressure coefficient, which is obtained by using the Rowe's theory. Consequently the values of $(Ka)_M$ thus obtained are governed mainly by the intensity of the vibrations.

$$(K_a)_M = M / \gamma H^3 \tau \tag{4}$$

where

$$\tau = f(\alpha, \beta, \delta, m_f, \varepsilon)$$

In Fig.5 the values of $(Ka)_M$ obtained from various values of measured bending moments are plotted against to the accelerations of the table. Also the earthpressure coefficient in an earthquake obtained by the seismic coefficient method is shown in the figure for the comparison. The method is so called Mononobe-Okabe formula and it gives the expression for the earthpressure coefficient as follows.

$$K_a = \frac{\cos^2(\phi - \varepsilon)}{\cos\varepsilon \cos(\delta + \varepsilon)\left[1 + \sqrt{\frac{\sin(\phi + \delta)\sin(\phi - \varepsilon)}{\cos(\delta + \varepsilon)}}\right]^2} \tag{5}$$

where ϕ is the angle of internal friction, δ the angle of the wall friction, $\tan\varepsilon = k_h$ and k_h is the horizontal seismic coefficient.

Measured values of $(Ka)_M$ are smaller by 20 ~ 30% than that calculated by the above formula. It is seen that large values of $(Ka)_M$ are obtained in the cases of heavy models. From this figure, it can be recognized that the increase in the maximum bending moment during vibrations is not remarkable, owing to the flexibility of the wall, as in the state without vibrations. The values of the soil stiffness modulus obtained by this way always decrease with increasing intensity of the vibration.

This will be mentioned later.

(2) Earthpressure

The earthpressure acting against the wall is obtained by the theory of the beam from the distribution of the bending moment.[4] In Figs.6 (1), (2), (3), (4) and Figs.7 (1). (2), (3), (4), (5) the representative examples of the distribution of earthpressure are illustrated. The earthpressures during vibrations are extremely large in the vicinity of the anchor level and do not increase much in the middle part of the span owing to the redistribution of the earthpressure due to the movement of the wall. The phase of the earthpressure in a vibration is same as that of the wall movement in the vicinity of the anchor level and the dredge level, but is reverse in the middle part of the span. In order to investigate the change of the earthpressure with the intensity of the vibration, it is convenient to use the coefficient of total earthpressure obtained by the following equation as shown in Fig.3.

$$K_a = \frac{2P}{(1+2\beta)\gamma H^2} \qquad (6)$$

where P is the total earthpressure. From Fig.3, it can be recognized that the measured earthpressures are smaller than the values by the M-O Formula except for the cases of the heavy walls (the A1-1 wall mounted the pressure cells), and the application points of the total earthpressure do not change remarkably with the intensity of vibrations.

(3) Subgrade reaction

The values of the subgrade reaction obtained by the measured values of the bending moment are compared with the values calculated by the Rowe's theory in Figs.6 and 7. It can be seen that the calculated values compare favourably with general tendency of the distribution of the subgrade reaction.

The values of the soil stiffness modulus do not change for cases with or without the surcharge load. The value of the soil stiffness modulus without vibration is governed mainly by the density of the sand and the amount of the wall movement, and it has been shown by Rowe[5] that the value is inversely proportional to 0.5 power of the angle of the wall rotation θ_d at the dredge level. In the present experiments, as shown in Fig.8, m values are inversely proportional to 1.5 ~ 2 power of the values θ_d. Therefore, this fact shows that the values of the soil stiffness modulus decrease with increasing intensity of vibration.

Since the wall movement is considerably large in the vicinity of the dredge level, the passive earthpressure is fully mobilized. The passive earthpressure line by M-O Formula is drawn in Figs.6 and 7, the ϕ value being chosen corresponding to the density of sand from the shear box test results. The value of the angle of the wall friction is found to be considerably large and its value is $2\phi/3$ in the present test.

(4) Movement of the wall

As for the movement of the wall, the portion which increases statically with increasing intensity of the vibration is remarkably large and the oscillating portion is extremely small. The oscillating portion is in same phase as the movement of the table and the magnitude of the oscillating movement is approximately proportional to the height of the wall. The distribution of the statically increasing portion of the wall movement is represented approximately by the Rowe's theory as shown in Figs.6 and 7.

(5) Anchor load

The anchor load also consists of two portions, statically increasing portion with the increase in the intensity of the vibration is comparatively large and also the oscillating portion is large owing to the condition of no anchor yield. For the sake of convenience the measured values of the anchor load are represented in the following form of $(Ka)_T$ as in the case of the bending moment and plotted against the accelerations of the table. (Fig.9)

$$(K_a)_T = T/\gamma H^3 \lambda \qquad (7)$$

where

$$\lambda = f(\alpha, \beta, \varphi, m\varphi, \varepsilon)$$

and T is the total anchor load.
Fig.9 shows, that the measured values are larger than the values calculated by the M-O Formula, and not influenced by the weight of walls. It is considered that the remarkable increase in the anchor load is caused mainly by the increase in the earthpressure in the vicinity of the anchor level during vibration.

Solitary vibration

When the solitary vibration is given to the table, the high-frequency vibration due to the properties of the apparatus appears as shown in Figs. 11 (1), (2). The frequency and the acceleration of the high-frequency vibration are 13c/s and 480 gal respectively, and the frequency characteristics of the structure as well as the effects of the duration of vibration can be investigated by examining this vibration. The test conditions shown in Fig.11 are nearly equal to the conditions of the test of A1-3. (Fig.6), and the distributions of the bending moment of that test are shown in Fig.10. From these figures it can be recognized that the maximum value of the bending moment in the case of the 480 gal in solitary vibration is nearly equal to the value in the case of the 250 gal increasing vibration. However, the bending moments at the upper and lower supports and the anchor load in the solitary vibration are considerably larger than in the increasing vibration.

By considering above mentioned facts, it can be recognized that the behaviour of the anchored sheet-pile wall in a vibration is less influenced by the frequency characteristics, but much influenced by the intensity and the duration of vibration. If the anchored sheet-pile wall is subjected to vibrations of the same acceleration, the effect of shorter vibration may be about a half of that of longer vibration.

Considerations on Results of Experiments

Since the dynamic properties of dry sand are governed mainly by the internal friction, the behaviour of sand in a vibration seems to be explained by the concept of the seismic coefficient method in the first approximation. It is tried to analyse the stresses in the semi-infinite sand stratum under an action of horizontal body force, in particular, with reference to the decrease of the subsoil stiffness.

Here, let it be assumed that the semi-infinite dry sand stratum is subjected to the forced vibration due to the horizontal displacement by some means. Neglecting the relative displacements of the sand and the term of time, and assuming Mohr-Coulomb's criterion, the equations of stress equilibrium are expressed as follows.

$$\frac{\partial \sigma_x}{\partial x} + \frac{\partial \tau_{xy}}{\partial y} = \gamma , \qquad \frac{\partial \tau_{xy}}{\partial x} + \frac{\partial \sigma_y}{\partial y} = k_h \gamma \tag{8}$$

and

$$\left.\begin{matrix}\sigma_x \\ \sigma_y\end{matrix}\right\} = \sigma(1 \pm \sin\phi\cos 2\theta) , \quad \tau_{xy} = \sigma \sin\phi \sin 2\theta \tag{9}$$

where $k_h = \tan\varepsilon$ is the seismic coefficient.
Substituting Eq.(9) to Eq.(8) and assuming the straight slip line, the following equations are obtained.

$$\begin{cases} (1+\sin\phi\cos 2\theta)\dfrac{\partial \sigma}{\partial x} + \sin\phi\sin 2\theta \dfrac{\partial \sigma}{\partial y} = \gamma \\ \sin\phi\sin 2\theta \dfrac{\partial \sigma}{\partial x} + (1-\sin\phi\cos 2\theta)\dfrac{\partial \sigma}{\partial y} = k_h \gamma \end{cases} \tag{10}$$

Under the condition of the uniform surcharge or no surcharge, the following expression is obtained.

$$\frac{dy}{dx} = -\frac{\partial\sigma/\partial x}{\partial\sigma/\partial y} = \frac{(1-\sin\phi\cos 2\theta) - k_h \sin\phi\sin 2\theta}{\sin\phi\sin 2\theta - k_h(1+\sin\phi\cos 2\theta)}$$

The condition of horizontal surface leads to,

$$\sin\phi\sin 2\theta - k_h(1+\sin\phi\cos 2\theta) = 0$$

$$\varphi = \frac{1}{2}\left\{\varepsilon + (1-n)\frac{\pi}{2} + n\sin^{-1}\frac{\sin\varepsilon}{\sin\phi}\right\} \qquad (11)$$

$$(n = \pm 1)$$

where the positive sign corresponds to the active state and the negative to the passive state. If there is no surcharge, the expression for mean normal stresses becomes

$$\bar{\sigma} = \frac{\cos\varepsilon \mp \sqrt{\sin^2\phi - \sin^2\varepsilon}}{\cos^2\phi\cos\varepsilon}\gamma x \qquad (12)$$

Then, the stress components are obtained as follows.

$$\begin{aligned} \sigma_x &= \gamma x \\ \sigma_y &= \begin{cases} \gamma x\left(\dfrac{1+\sin^2\phi}{1-\sin^2\phi} - \dfrac{2}{\cos\phi}\sqrt{\tan^2\phi - \tan^2\varepsilon}\right) \\ \gamma x\left(\dfrac{1+\sin^2\phi}{1-\sin^2\phi} + \dfrac{2}{\cos\phi}\sqrt{\tan^2\phi - \tan^2\varepsilon}\right) \end{cases} \\ \tau_{xy} &= \gamma x\tan\varepsilon \end{aligned} \qquad (13)$$

All values of the stress components are independent on the signs of k_h . The values of the mean normal stress $\bar{\sigma}$ in the active state increase with increasing value of k_h , on the other hand, the values of $\bar{\sigma}$ in the passive state decrease with increasing value of k_h . Since the soil stiffness modulus is defined as the degree of the mobilization of the ϕ value in the passive state, it is considered that this fact gives a qualitative explanation to the decrease of the soil stiffness modulus with the increasing intensity of vibrations.

When the value of angle ε equals to the angle of internal friction in Eq.(13), the following coefficient of earthpressure is obtained.

$$\frac{\sigma_y}{\sigma_x} = \frac{1+\sin^2\phi}{1-\sin^2\phi} \qquad (14)$$

The same coefficient was obtained by Bent Hansen[6] as the stress state at failure in the box shear test. Hence, it may be considered that the vibration box test is somewhat similar with the box shear test.

Though the soil stiffness decreases during vibrations, the degree of fixity of the embedded portion may increase, if the values of m_ϕ are larger than a definite value as mentioned in the previous chapter. And even if the values of m_ϕ are smaller than a definite value, there is a considerable margin for safety on the degree of fixity of the embedment.

Since the large amount of loads acts on the anchorage during vibrations, it is the most important point in the earthquake resistant design of anchored sheet-pile walls to reduce the loads acting on the anchorage and to give a sufficient resistance to the anchorage for safety.

As the anchored sheet-pile bulkheads mostly exist in water, the dynamic effects of water, which are expressed in terms of the apparent seismic coefficient and the dynamic water pressure acting on the wall, may be the main factor on the seismic stability of retaining structures. However those effects are not taken into consideration in the present paper, since the conclusive test results have not been obtained yet.

Conclusion

As already mentioned, there are many unknown problems in the present model test, but it may be said that the general characteristics of anchored sheet-pile walls in vibration has been disclosed to a certain extent. As comparing with the results of test without vibration, the results of the present test are different on the following points.

(1) The influences of vibration are remarkable, in particular, at the anchorage and embedment.

(2) The earthpressure during vibration becomes large increasingly toward the elevation of anchorage, hence the anchor load also becomes large remarkably.

(3) The soil stiffness during vibration decreases with the increasing intensity of vibration, but it seems that there is a considerable margin for safety on the degree of fixity of the embedment.

The results of the present test would give a useful knowladge for the earthquake resistant design of anchored sheet-pile bulkheads.

Bibliography

(1) R. Amano, H. Azuma and Y. Ishii: Aseismic Design of Quay-Walls in Japan. Proc. 1st World Conference on Earthquake Engineering, 1956.
(2) Y. Ishii, H. Arai and H. Tsuchida: "Lateral Earthpressure in an Earthquake." Proc. 2nd World Conference on Earthquake Engineering, 1960.
(3) P.W. Rowe: "A Theoritical and Experimental Analysis of Sheet-pile Walls." Proc. I.C.E. Vol.4, Pt.1, 1955.
(4) G.P. Tschebotarioff: "Soil Mechanics, Foundation and Earth Structures." 1951.
(5) P.W.Rowe: "The Single Pile Subjected to Horizontal Force." Geotechnique, Vol.6, No.2, 1956.
(6) Bent Hansen: "Shear Box Test on Sand." Proc. 5th Int. Conf. Soil Mech. and Foundation Eng., 1961.

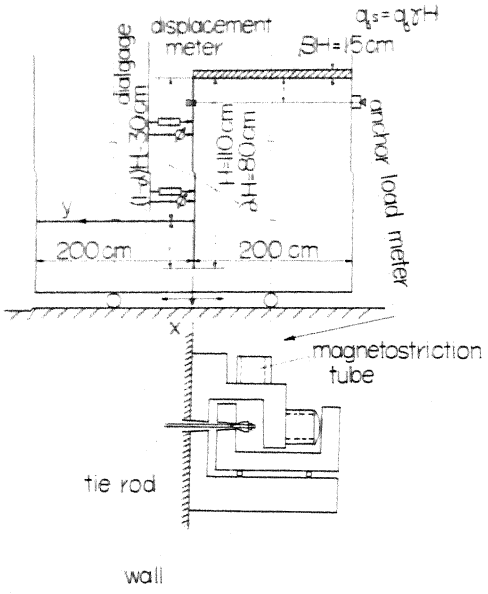

Fig.1 Schematic Diagram of Experiment.

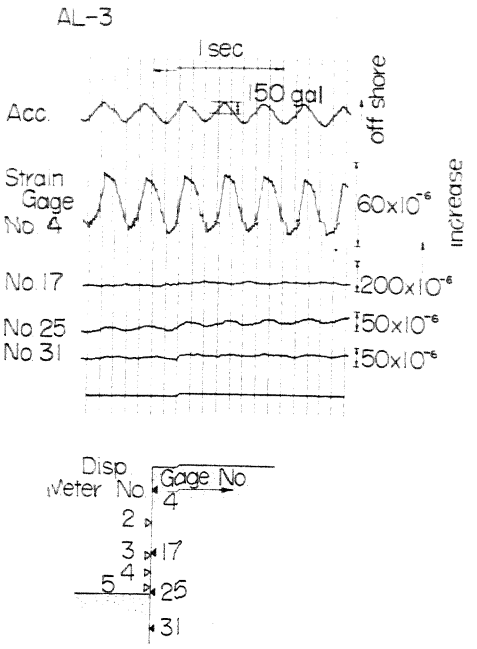

Fig.2-(1) Strain Records during Increasing Vibration.

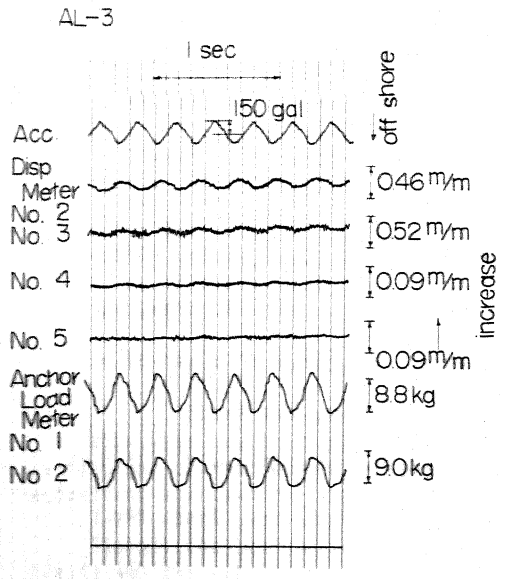

Fig.2-(2) Records of Displacement of Wall and Auchor Load during Increasing Vibration.

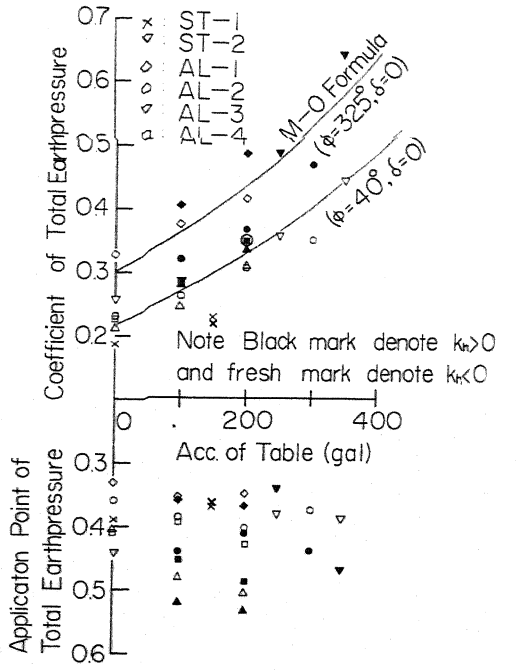

Fig.3 Relation between Earthpressure Coefficient and Acceleration of Table.

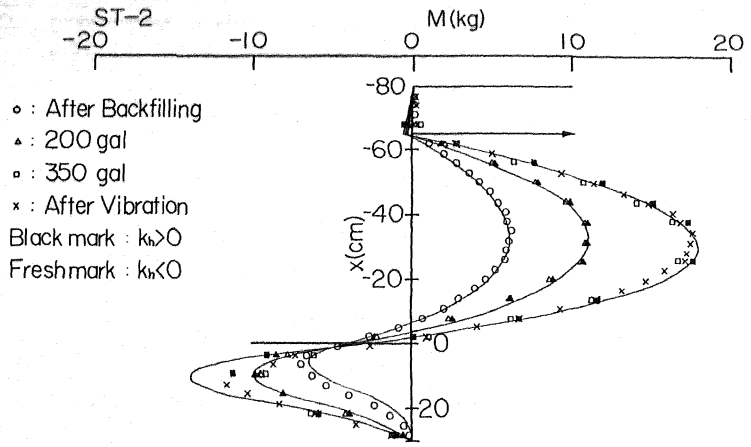

Fig.4-(1) Distribution of Bending Moment.

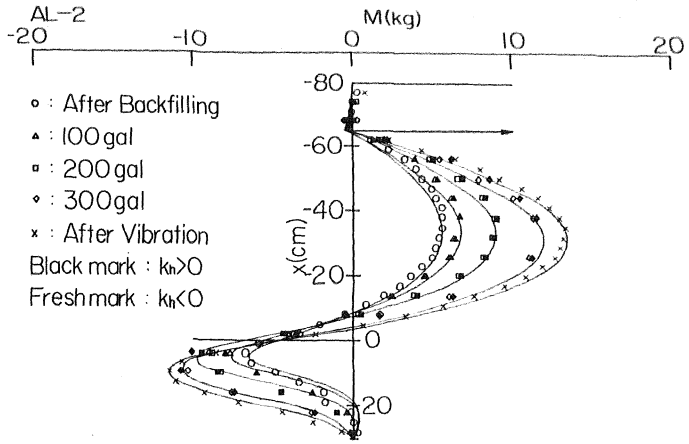

Fig.4-(2) Distribution of Bending Moment.

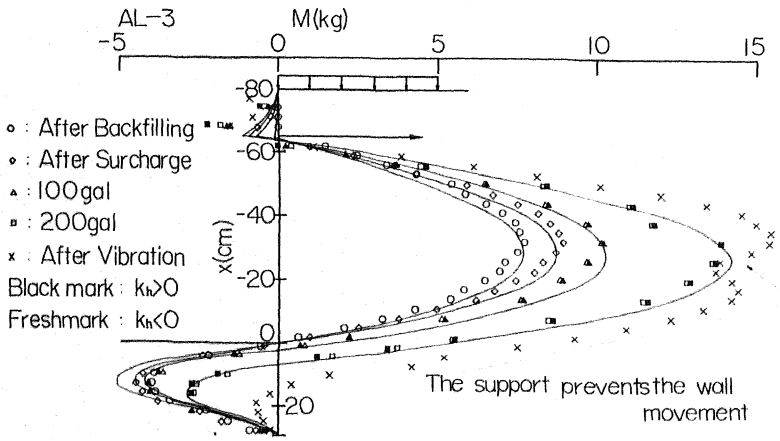

Fig.4-(3) Distribution of Bending Moment.

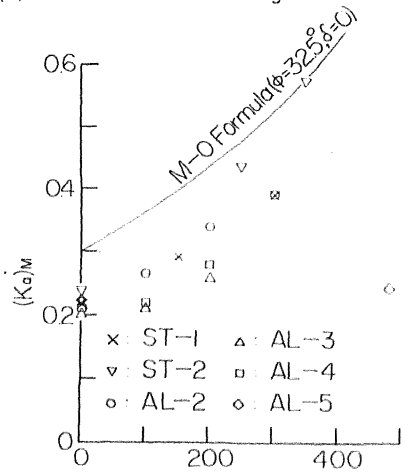

Fig.5 Relation between Modefied Earthpressure Coefficient and Acceleration of Table

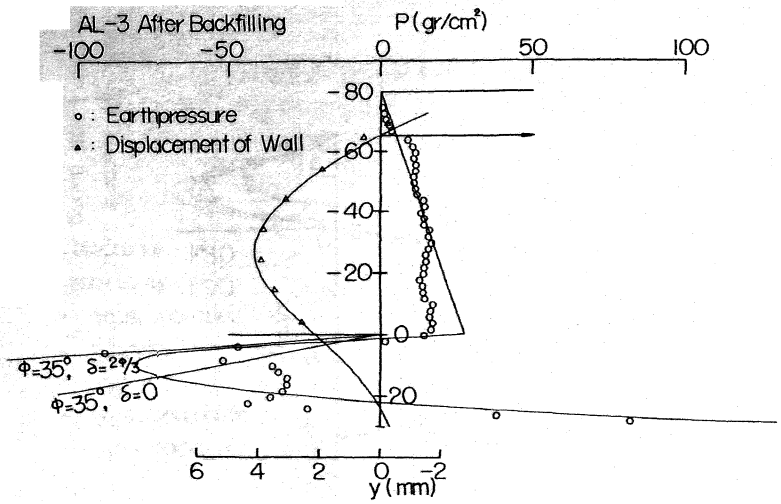

Fig.6-(1) Distribution of Earthpressure and Displacement of Wall.

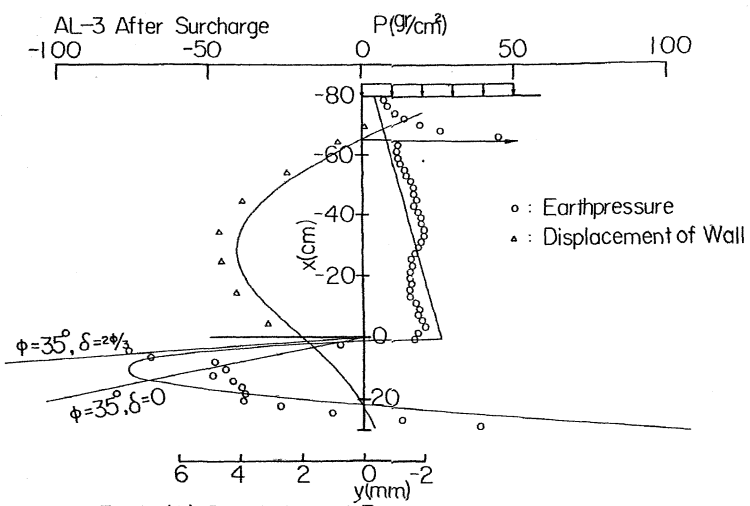

Fig.6-(2) Distribution of Earthpressure and Displacement of Wall.

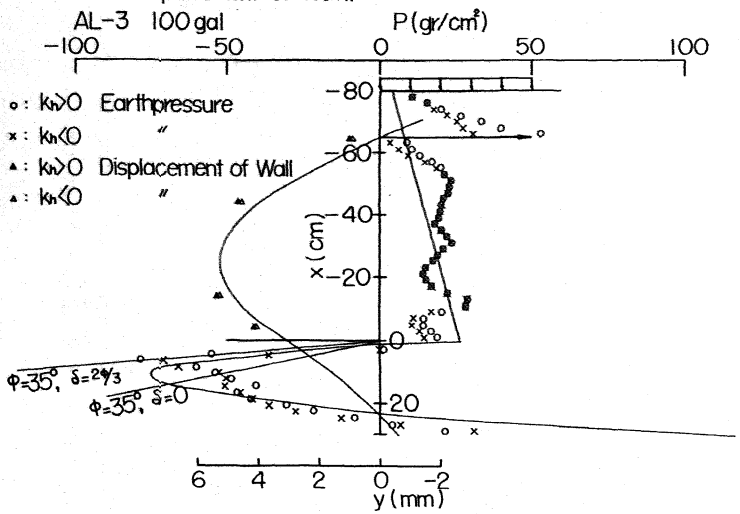

Fig.6-(3) Distribution of Earthpressure and Displacement of Wall.

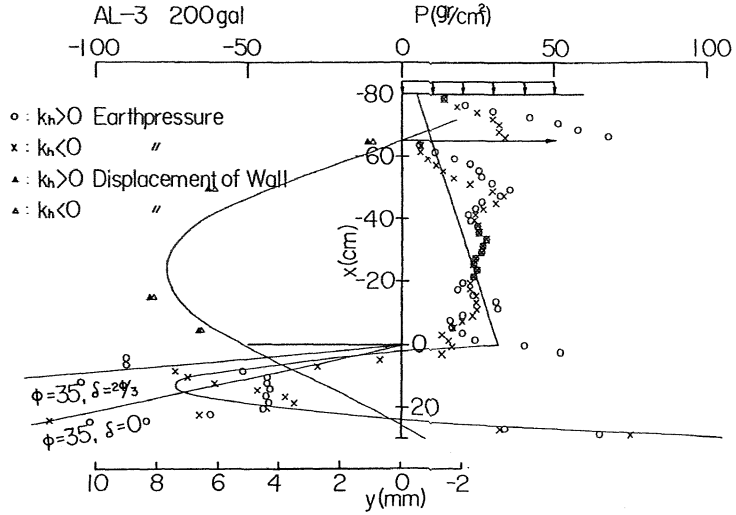

Fig.6-(4) Distribution of Earthpressure and Displacement of Wall.

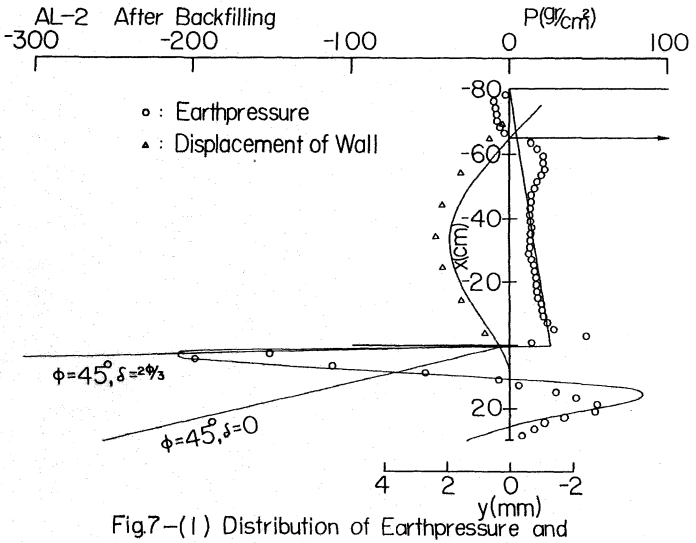

Fig.7-(1) Distribution of Earthpressure and Displacement of Wall.

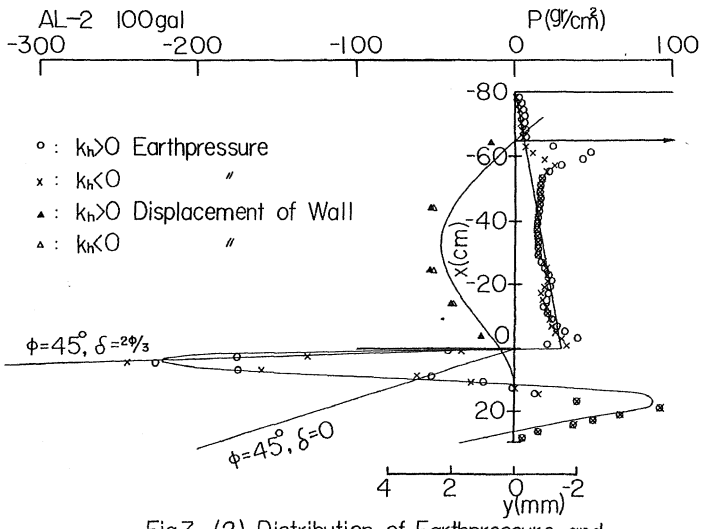

Fig.7-(2) Distribution of Earthpressure and Displacement of Wall.

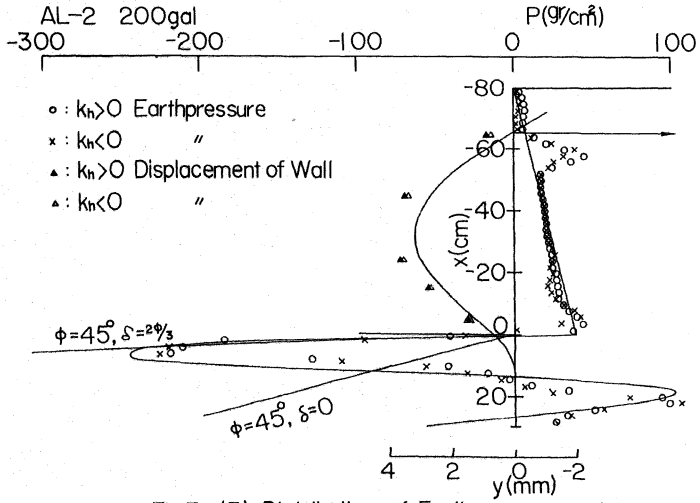

Fig.7-(3) Distribution of Earthpressure and Displacement of Wall.

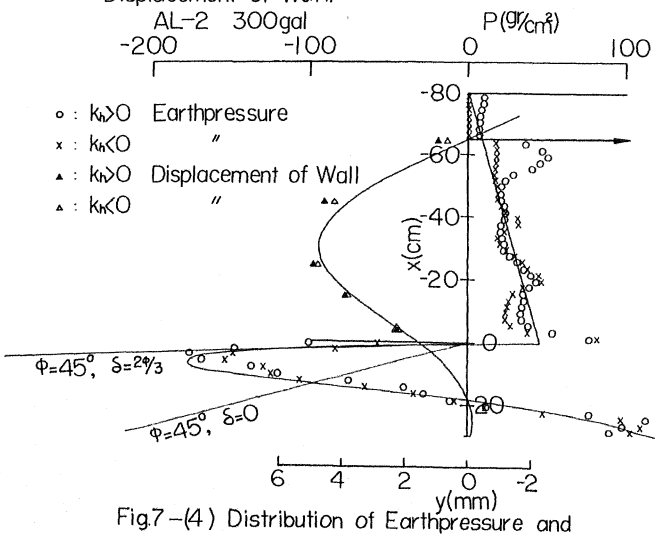

Fig.7-(4) Distribution of Earthpressure and Displacement of Wall.

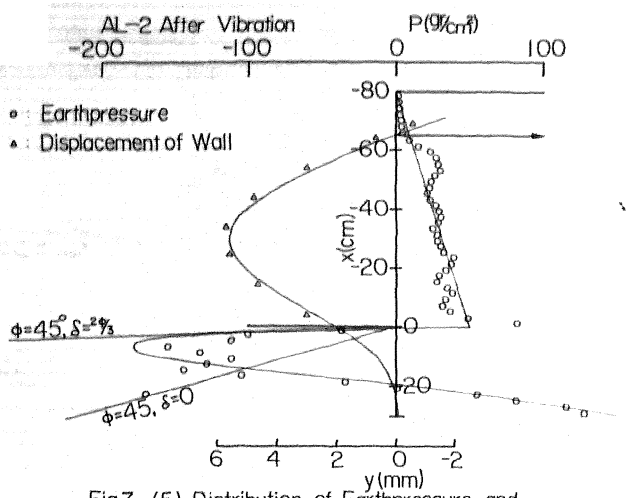

Fig.7-(5) Distribution of Earthpressure and Displacement of Wall

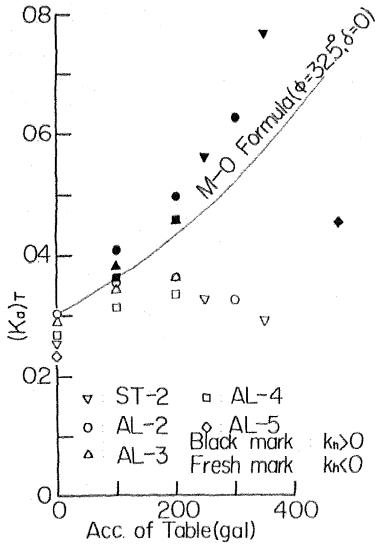

Fig.9 Relation between Modified E.P. Coefficient and Acc. of Table.

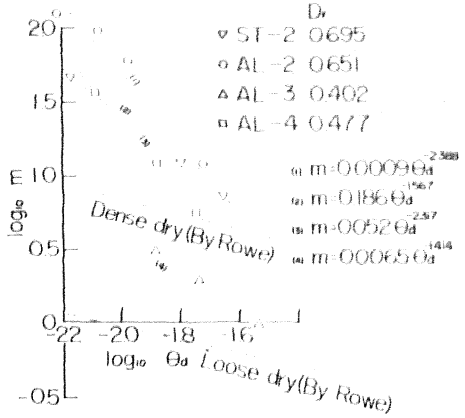

Fig. 8 Relation between Soil Stiffness Modulus and Rotation Angle of Wall at Dredge Level.

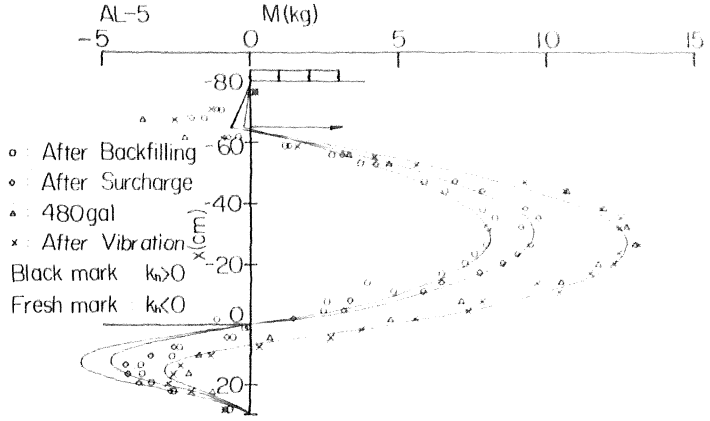

Fig. 10 Distribution of Bending Moment

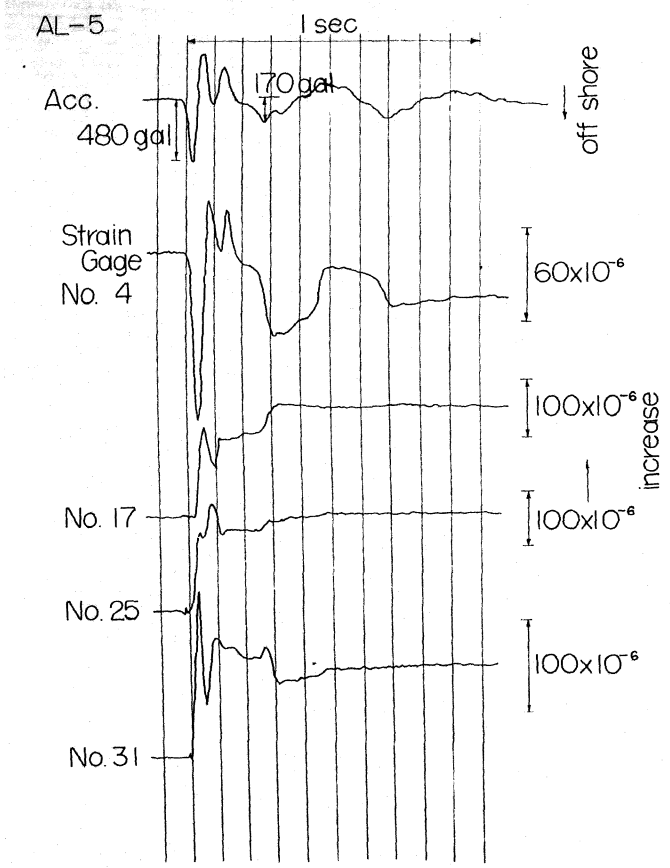

Fig. 11-(1) Strain Records during Solitary Vibration.

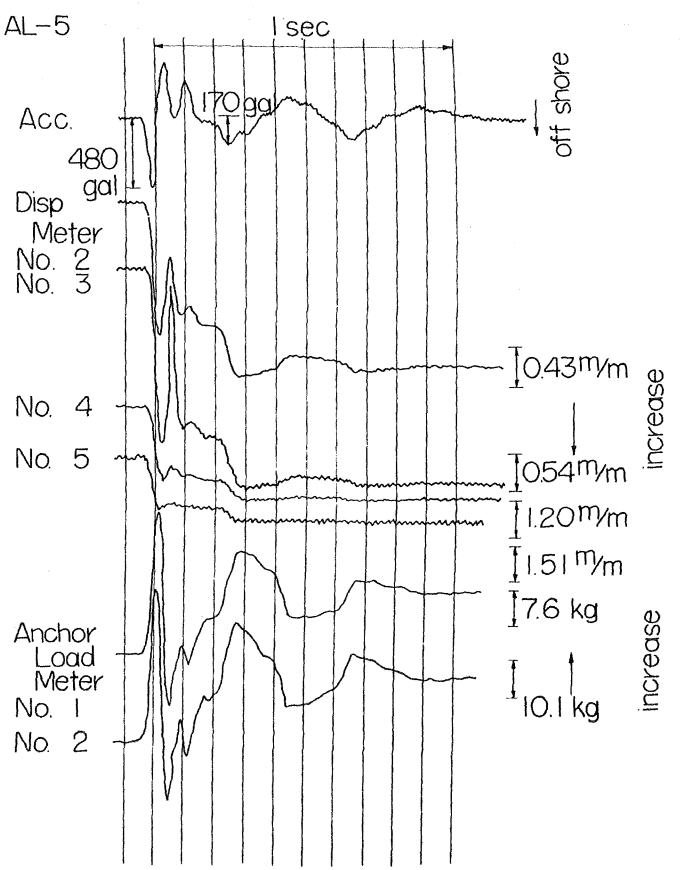

Fig. 11-(2) Records of Displacement of Wall and Anchor Load during Solitary Vibration.